NeuroImage: Clinical 16 (2017) 132–141

Contents lists available at ScienceDirect

NeuroImage: Clinical

journal homepage: www.elsevier.com/locate/ynicl

Resting-state functional connectivity changes due to acute and short-term valproic acid administration in the baboon model of GGE

Felipe S. Salinas[a,b,*], Charles Ákos Szabó[c,d]

[a] Research Imaging Institute, UT Health, San Antonio, United States
[b] South Texas Veterans Health Care System, San Antonio, TX, United States
[c] Department of Neurology, UT Health, San Antonio, United States
[d] South Texas Comprehensive Epilepsy Center, UT Health, San Antonio, United States

ARTICLE INFO

Keywords:
Resting-state fMRI
Genetic generalized epilepsy
Functional connectivity
Treatment effects
Animal models

ABSTRACT

Resting-state functional connectivity (FC) is altered in baboons with genetic generalized epilepsy (GGE) compared to healthy controls (CTL). We compared FC changes between GGE and CTL groups after intravenous injection of valproic acid (VPA) and following one-week of orally administered VPA. Seven epileptic (2 females) and six CTL (3 females) baboons underwent resting-state fMRI (rs-fMRI) at 1) baseline, 2) after intravenous acute VPA administration (20 mg/kg), and 3) following seven-day oral, subacute VPA therapy (20–80 mg/kg/day). FC was evaluated using a data-driven approach, while regressing out the group-wise effects of age, gender and VPA levels. Sixteen networks were identified by independent component analysis (ICA). Each network mask was thresholded ($z > 4.00$; $p < 0.001$), and used to compare group-wise FC differences between baseline, intravenous and oral VPA treatment states between GGE and CTL groups. At baseline, FC was increased in most cortical networks of the GGE group but decreased in the thalamic network. After intravenous acute VPA, FC increased in the basal ganglia network and decreased in the parietal network of epileptic baboons to presumed nodes associated with the epileptic network. After oral VPA therapy, FC was decreased in GGE baboons only the orbitofrontal networks connections to the primary somatosensory cortices, reflecting a reversal from baseline comparisons. VPA therapy affects FC in the baboon model of GGE after a single intravenous dose—possibly by facilitating subcortical modulation of the epileptic network and suppressing seizure generation—and after short-term oral VPA treatment, reversing the abnormal baseline increases in FC in the orbitofrontal network. While there is a need to correlate these FC changes with simultaneous EEG recording and seizure outcomes, this study demonstrates the feasibility of evaluating rs-fMRI effects of antiepileptic medications even after short-term exposure.

1. Introduction

Valproic acid (VPA) is the gold standard for antiepileptic treatment of genetic generalized epilepsies (GGE)—previously referred to as idiopathic generalized epilepsy (Löscher, 2002; Perucca, 2002). VPA is effective for the treatment of all generalized seizures types including absence, myoclonic and generalized tonic-clonic seizures (GTCS), but has also been shown to reduce interictal epileptic discharge (IED) rate and suppress photosensitivity (Harding et al., 1997; Sundqvist et al., 1999). The anticonvulsant effects of VPA are multiple: blocking voltage-gated sodium channels; blocking low-threshold calcium channels—which are essential to the generation of thalamic oscillations (and subsequently for the synchronization of the cerebral hemispheres); facilitating glutamatergic neurotransmission; reducing serotonin reuptake; and increasing overall GABA concentration in the CNS to name a few (Löscher, 2002). Furthermore, a recent scalp EEG study in people with GGE (Clemens et al., 2014) suggested that VPA also has network-wide effects, as evidenced by a frequency-dependent reduction in the functional connectivity (FC) of potentially epileptogenic networks and the restoration of physiological connectivity.

By measuring blood oxygen level dependent (BOLD) changes linked to electrophysiological activity—including interictal epileptic discharges (IEDs)—functional MRI (fMRI) may play a key role in our evolving understanding of the mechanisms underlying GGE (Benuzzi et al., 2012; Kay et al., 2013). Although EEG-fMRI demonstrates significant regional blood flow changes occurring before, during and after generalized spike-and-wave complexes, it is unclear to what extent FC varies between IEDs and IED-free periods in human GGE. Similar to its

* Corresponding author at: Research Imaging Institute, UT Health San Antonio, 7703 Floyd Curl Drive, San Antonio, TX 78229-7883, United States.
E-mail address: salinasf@uthscsa.edu (F.S. Salinas).

http://dx.doi.org/10.1016/j.nicl.2017.07.013
Received 7 February 2017; Received in revised form 14 July 2017; Accepted 15 July 2017
Available online 24 July 2017

Table 1
Demographics with VPA doses and levels. Legend: kg = kilogram; mg = milligram; mcg/ml = micrograms per milliliter; i.v. = intravenous; IED = interictal epileptic discharges; SZ = seizures; PS = photoparoxysmal or photoconvulsive responses; S.D. = standard deviation.

Animal #		Age (years)	Gender	Weight (kg)	Clinical seizures	EEG			VPA intravenous dose (mg)	Acute VPA level (mcg/ml)	VPA maintenance dose (mg)	Subacute VPA level (mcg/ml)
						IED	SZ	PS				
Control baboons	1	12	F	16	No	No	No	No	250	59	250	6
	2	10	F	15	No	No	No	No	250	92	250	13
	3	5	M	15	No	No	No	No	370	97	1000	10
	4	4	M	15	No	No	No	No	298	85	500	8
	5	9	M	24	No	No	No	No	380	80	750	11
	6	4	F	15	No	No	No	No	210	85	1000	21
	Mean ± S.D.	7 ± 4	–	17 ± 4	–	–	–	–	315 ± 108	86 ± 18	625 ± 345	13 ± 6
Epileptic baboons	1	3	M	11	Yes	Yes	Yes	No	250	74	250	5
	2	10	F	12	No	Yes	Yes	Yes	250	99	250	19
	3	10	M	30	Yes	Yes	Yes	No	250	52	500	9
	4	8	M	28	Yes	Yes	No	No	250	51	500	18
	5	15	F	18	Yes	Yes	No	No	360	82	250	19
	6	9	M	31	Yes	Yes	Yes	No	620	95	1250	6
	7	9	M	31	Yes	Yes	No	Yes	620	93	2500	16
	Mean ± S.D.	9 ± 4	–	23 ± 9	–	–	–	–	345 ± 144	78 ± 20	786 ± 835	15 ± 7

application in the assessment of treatment effects in major depressive disorder (Yang et al., 2014; Wang et al., 2015), rs-fMRI may also provide a platform to evaluate the network effects of antiepileptic medications in focal or generalized epilepsies, however there are only a few studies to date (Haneef et al., 2015; Hermans et al., 2015). Short-term modulation of brain networks has been demonstrated in healthy human subjects (taking diazepam for only a week), as well as in people with focal epilepsies withdrawing from antiepileptic medications (Pflanz et al., 2015; Hermans et al., 2015). But central to the question about whether antiepileptic medications affect FC, are the impact of transient fluctuations in BOLD signal related to ictal or interictal epileptic discharges, and the extent to which suppression of the discharges can normalize the FC (Centeno and Carmichael, 2014). Nonetheless, FC may be utilized as a biomarker for antiepileptic treatment effects. While this type of study could be conducted in people with newly diagnosed epilepsy, the need to involve children, the difficulty to dose and control compliance in this population, the need for rapid access to functional neuroimaging and repeat studies, and the cost to recruit a large number of subjects to overcome the challenges of anatomical and neurobehavioral variability could be offset by a similar study in an appropriate animal model.

The baboon model of GGE has a peak onset in adolescence and is characterized by absence, myoclonic and GTC seizures; these effects are usually witnessed during morning hours (or upon awakening) and are closely associated with photosensitivity (Szabó et al., 2011; Szabó et al., 2012a; Szabó et al., 2013). Hence, the baboon model of GGE closely resembles the human phenotype of juvenile myoclonic epilepsy (JME). As it shares a similar brain anatomy—both structurally and functionally—our group developed a platform for studying resting-state FC and photosensitivity in the epileptic baboon (Szabó et al., 2008; Szabó et al., 2011; Salinas and Szabó, 2015). The epileptic baboon, similar to human GGE, demonstrates a mixture of increased and decreased BOLD changes in cortical and subcortical brain regions between and during ictal or interictal epileptic discharges, which has not been documented in other GGE models so far (Youngblood et al., 2015). Despite the use of a low-dose ketamine infusion for sedation, this preparation reproduces several important physiological networks discovered in humans (including the default mode network), providing the opportunity to evaluate network responses to antiepileptic medications that have been shown to be effective in human GGE (Salinas and Szabó, 2015).

In this study, rs-fMRI was utilized not only to compare FC between medication-naïve epileptic (GGE) and healthy control (CTL) baboons, but also to compare FC changes in both groups 1) after acute intravenous administration of VPA and 2) following one-week of orally administered VPA. As VPA may alter global and regional cerebral blood flow—even in healthy controls (Gaillard et al., 1996)—we compared FC changes for each group by comparing each subject's treatment condition to their own pre-treatment baseline. Thus, the effects of VPA dose on the FC of specific brain networks were compared by assessing each the FC changes of each group's response to VPA dose. We hypothesized that this effect would be demonstrated more profoundly after sustained (i.e. subacute) exposure to VPA rather than after an acute VPA dose. We also expected that subacute VPA treatments would not only revert the FC abnormalities observed in brain networks involved in GGE, but may also "normalize" some of these networks to the FC distributions observed in the pre-treatment CTL group. By demonstrating the feasibility of measuring these FC changes related to antiepileptic medications, and eventually linking these to therapeutic efficacy, rs-fMRI may become established as a tool for the development and testing of new antiepileptic therapies (both in animals and humans).

2. Materials and methods

2.1. Animal selection

Using clinical and EEG data we identified 20 baboons (*Papio hamadryas anubis* and its hybrids; 11 GGE/9 CTL; 9 females), with the mean (± standard deviation) age of 9 ± 5 years old, that were housed at the Southwest National Primate Research Center (SNPRC), part of the Texas Biomedical Research Institute (TBRI), in San Antonio, Texas. Clinical data was obtained from CAMP, the veterinary database used at the SNPRC. All of the GGE baboons either had a clinical history of witnessed seizures or exhibited seizures during the scalp EEG study (Table 1). Scalp EEG studies were performed at UT Health San Antonio and details of the procedure have been described previously (Szabó et al., 2013). All of the baboons were lightly sedated with intramuscular ketamine 5–6 mg/kg, for transfer to a primate chair and placement of scalp electrodes. During each study, photic stimulation was performed at frequencies ranging from 3 to 30 Hz (on two occasions, fifteen minutes apart), to establish the presence or absence of photoparoxysmal or photoconvulsive responses. Intramuscular ketamine (5–6 mg/kg) was repeated for removal of the electrodes and transfer of the baboon back to its cage. A neurologist (CÁS), who is board-certified in epilepsy and clinical neurophysiology, interpreted all scalp EEG studies.

Of the 20 baboons, 6 were eliminated after they were found to have structural MRI anomalies, including 1) occipital horn elongation(s) extending posteriorly beyond the mesiobasal origin of the calcarine sulcus, or 2) occipital horn enlargement (i.e. colpocephaly; (Szabó et al., 2016). One additional male was removed after an idiosyncratic

response to ketamine. The thirteen remaining baboons (7 GGE/6 CTL, 5 females) had a mean age of 8 ± 4 years old (Table 1). All seven GGE (2 females) baboons demonstrated IEDs on scalp EEG, but only two had photoparoxysmal responses. None of the six (3 females) CTL animals had ictal or interictal EEG abnormalities. There were no significant differences in age or weight between the GGE and CTL groups.

All animals were studied in accordance with the policies of the Institutional Animal Care and Use Committee of the UT Health San Antonio; this study fully complied with the National Research Council's *Guide for the Care and Use of Laboratory Animals* (National Research Council, 2011) and the U.S. Public Health Service's *Animal Welfare Act* (U.S. Public Health Service, 2009). Principles outlined in the ARRIVE guidelines and in the Basel declaration (http://www.basel.declaration.org) were considered when designing the study.

2.2. VPA administration

Intravenous VPA (20 mg/kg) was administered during the first MRI session after the completion of each animal's first functional study, achieving serum levels of 80 ± 17 mcg/ml at a mean of 59 ± 4 min following administration; we will refer to the first scan as each animal's "baseline" scan. The functional study was repeated within 40 min of VPA administration; we will refer to this scan as each animal's "acute VPA" scan. All baboons began a daily oral maintenance dose of 20–80 mg/kg on the night of the first MRI session. Due to the low trough VPA levels after seven days of VPA administration in the first few baboons that completed the study, the maintenance doses were increased in subsequent animals. The mean trough dose (drawn prior to the final scan) after seven days was 12 ± 6 mcg/ml. A final fMRI study was performed after this seven-day VPA treatment; we will refer to this scan as each animal's "subacute VPA" scan. There were no significant differences in either of the VPA levels between the GGE and CTL groups.

2.3. Resting-state fMRI

The anesthetized animal preparation—for optimized physiological stability and functional imaging responses—has been described in previous studies (Szabó et al., 2008; Salinas and Szabó, 2015). Briefly, for each rs-fMRI scan, the animal received an injection of intramuscular ketamine (5 mg/kg) to facilitate oral intubation and catheterization of a venous delivery line; intramuscular atropine (0.3 mg) was administered to reduce oropharyngeal secretions. During each imaging session, we maintained sedation with continuous i.v. administration of ketamine (5–6 mg/kg/h), which simulated the dose utilized for the scalp EEG recording, and vecuronium (0.25 mg/kg/h)—a paralytic that acts at the neuromuscular junction. Upon conclusion of the imaging session, we administered atropine (0.6–1.2 mg, i.v.) and neostigmine (0.5–2.0 mg, i.v.) to reverse muscle paralysis. During the entire procedure, the animals' respiration, heart rate and oxygenation were monitored. With the exception of the one male baboon (described above), no complications were noted during or after any of the procedures.

The MRI scans were performed on a 3T Siemens TIM Trio clinical MRI scanner using a body radio-frequency transmission coil with a 12-channel head RF receiver coil (Siemens, Erlangen, Germany). BOLD rs-fMRI was acquired using a gradient echo-planar imaging pulse sequence. Whole brain coverage rs-fMRI was acquired parallel to the AC-PC line with the following scanning parameters: TR/TE = 3000/30 ms, acquisition matrix = 124 × 124 mm, spatial resolutions of 1.048 mm × 1.048 mm, and 27 axial slices (slice thickness = 1.9 mm) were acquired for at least five minutes. In the same session, high-resolution anatomical images were acquired using an MP-RAGE sequence (TR/TE/flip angle = 2100 ms/3.1 ms/12°), non-selective inversion pulse, TI = 1100 ms, FOV = 160 × 192 × 192 mm, 1.0 mm isotropic spatial resolution. We used the anatomical MRIs for within modality co-registration and spatial normalization.

2.4. Data preprocessing

Anatomical MRIs were preprocessed with the Brain Extraction Tool (BET; Smith, 2002) in the FMRIB's Software Library (FSL; Smith et al., 2004), to remove non-brain tissues. FSL's Fully Automated Segmentation Tool (FAST; Zhang et al., 2001) was used to segment the brain into white matter, gray matter and ventricular masks; a global (whole-brain) mask was created by combining each of these masks. The resulting images were used during the rs-fMRI preprocessing stages—developed in our previous study (Salinas and Szabó, 2015)—which we have briefly described below.

All rs-fMRIs were preprocessed using FSL's FMRI Expert Analysis Tool (FEAT; Woolrich et al., 2009). The initial rs-fMRI preprocessing steps include: removal of the first 4 volumes of rs-fMRI data for T1-equilibration, motion correction (using signal regression of 24 motion parameters), slice timing correction, and rs-fMRI brain extraction. The white matter and ventricular masks were eroded to 65% of their original volume to ensure that each mask was only sampling data from the respective brain region (Chai et al., 2012). Global white matter, and ventricular masks were then used to determine each baboon's nuisance signals. Initially, each animal's preprocessed dataset underwent nuisance regression using only the white matter and ventricular signal regressors (i.e. 2-covariates; Weissenbacher et al., 2009). To determine whether or not to include the global signal in nuisance regression, we implemented the global negative index (GNI; Chen et al., 2012) using in-house computer programs developed in MATLAB (Natick, MA, USA). The white matter and ventricular signal regression of each rs-fMRI then underwent isotropic spatial smoothing (FWHM = 6.0 mm), spatial normalization to a representative baboon brain, and band-pass filtering ($0.008 < f < 0.1$ Hz). A graphical display of our data processing pipeline is shown in Fig. 1.

2.5. Intrinsic connectivity networks

We performed independent component analysis (ICA) on all animal's (N = 13) baseline rs-fMRI scans using FSL's MELODIC program (Beckmann et al., 2005). The group-ICA was extracted using an automatic estimation of the components to determine the baboon's major brain networks. We repeated our ICA four more times to ensure that each of the resulting brain networks consisted of reproducible brain regions. The resulting brain networks were then thresholded ($z > 4.00$; $p < 0.001$) to make masks for each brain network; this threshold was only applied to our ICA results to determine each time-series, not to any of our functional connectivity differences described below. Once each brain network was determined, we used FSL's cluster

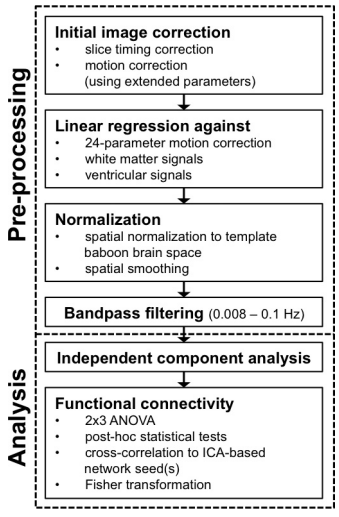

Fig. 1. Data processing pipeline.

analysis algorithm on each thresholded network to determine its major components. These brain regions were identified using homologous brain areas listed in Saleem & Logothetis' rhesus brain atlas (Saleem and Logothetis, 2007). The thresholded mask of each ICA-derived brain network was used to calculate each animal's network-specific time-series for functional connectivity analysis of the preprocessed datasets.

2.6. Functional connectivity analysis

Each animal's preprocessed rs-fMRI datasets (baseline, acute VPA, and sub-acute VPA scans) underwent voxel-wise, "first-level" analysis for each brain network's ICA-derived time-series—using FSL's FEAT program—to determine the FC of each group's respective brain network on each animal's respective dataset. Initially, we used a 2 × 3 analysis of variance (ANOVA) with Group (e.g. GGE or CTL) and VPA administration (e.g. baseline, acute VPA, subacute VPA) as factors, while regressing out any effects of gender, age, or VPA dosage. Only the brain networks which demonstrated significant ($p < 0.05$) F-tests for the Group × VPA Administration interaction were used for post hoc analyses to assess each animal's response to acute VPA and subacute VPA treatments (when compared to baseline). We used FEAT's "fixed effects" for our "mid-level" analysis to ensure that our variance was modeled accurately for each subject in the brain networks which demonstrated significant Group × VPA Administration interactions. We also assessed whether or not there was any normalization of FC in the altered GGE networks by comparing the "subacute VPA" scans in the GGE baboons with the "baseline" scans of the CTL group; these "mid-level" comparisons were also analyzed using a "fixed effects" analysis. Once all of our lower level (post hoc) analyses were performed, we applied FEAT's "higher-order" analysis—using the FMRIB's Local Analysis of Mixed Effects (also in FEAT) to determine any group-wise effects; we regressed out the effects of age, gender and VPA dose levels when performing these post hoc tests. These analyses produced contrasts between the CTL and GGE groups for: "baseline", "acute VPA vs. baseline", "subacute VPA vs. baseline", and "GGE subacute VPA vs. CTL baseline" scans in their respective networks. The resulting contrast images underwent threshold-free cluster enhancement using FSL's "randomise" command and were family-wise error (FWE) corrected. The resulting FWE-corrected images were then overlaid onto a representative baboon brain for visualization and region identification (Love et al., 2016). The full range of each group's respective functional connectivity map was used to determine the maximum and minimum z-scores for each brain network. Cluster analysis was performed on the contrast images (using FSL's algorithm) to determine each contrast image's major components. These brain regions were then identified using homologous regions in the rhesus brain (Saleem and Logothetis, 2007).

3. Results

There were no significant ($p < 0.05$) differences in the gender, age, weight or VPA dose levels between the GGE and CTL animals (summary demographics were reported in the Supplementary materials). An analysis of each subject's rs-fMRI scan's global-negative index determined that global signal regression should *not* be performed on any of our rs-fMRI scans—since its inclusion introduced more errors in our FC measurements; therefore, all of the rs-fMRI scans used in our analyses underwent motion correction (using signal regression of 24 motion correction parameters) and nuisance-regression for only the white matter and ventricular signals. ICA of the pre-processed baseline scans identified 16 brain networks—which were replicated in each of our five ICA iterations (Fig. 2).

Table 2 lists the intrinsic connectivity networks that demonstrated significant ANOVA results for the Group × VPA Administration interactions. Baseline FC differences were observed between the GGE and CTL groups in the pericingulate, precuneus, left parieto-occipital, parietal, orbitofrontal, temporo-parietal, secondary visual, and thalamic brain networks. FC differences between groups were observed after acute VPA administration in the basal ganglia, primary visual, and parietal brain networks. Subacute VPA administration demonstrated FC differences between groups in the orbitofrontal brain network. Comparison of the GGE animal's subacute VPA scans with the CTL group's baseline scans yielded significant FC differences in the perisylvian operculum and the fronto-parietal brain networks.

Post hoc testing demonstrated that FC differences between the GGE and CTL groups at baseline spread across eight brain networks (Table 3 and Fig. 3; see Supplementary materials for complete list of all clusters involved in this analysis). In many of these brain networks, FC was increased in the GGE group—e.g. in the pericingulate, default mode, left parieto-occipital, parietal, orbitofrontal, and secondary (basal) visual area—while decreases were observed in the temporo-parietal and thalamic brain networks. Overall, increases in the FC of these brain regions affected their respective connection to the visual cortices of the GGE animals. Overall, these ICA-derived brain networks (and their baseline differences between the GGE and CTL groups) are very consistent with our previously reported resting-state fMRI study in the baboon model of GGE (Salinas and Szabó, 2015).

Table 4 and Fig. 4 show the maximum cluster locations for our post hoc analysis of the FC differences between the "acute VPA vs. baseline" scans for the GGE and CTL groups; see Supplementary materials for complete list of all clusters involved in this analysis. After acute administration of intravenous VPA, the primary visual and parietal cortical networks demonstrated significant decreases in FC in GGE baboons compared to the CTL group, whereas FC was increased in the subcortical-cortical connections via the basal ganglia network.

Table 5 and Fig. 5 show the maximum cluster locations for the FC differences between the "subacute VPA vs. baseline" scans of the GGE and CTL groups. After administration of an intravenous load of VPA, followed by one-week of oral maintenance VPA therapy, FC increased in GGE baboons (compared to controls) only in the orbitofrontal network.

In order to evaluate any normalization of FC in the altered networks we compared the "subacute VPA" therapy scans in the GGE baboons with the "baseline" CTL group (Table 6 and Fig. 6). Even with subtherapeutic VPA levels achieved after the oral maintenance therapy, most network FC changes noted at baseline did not achieve statistical significance or these FC differences appeared to have been resolved. FC increases in the perisylvian opercular network and decreases in the frontoparietal network were not apparent at the pre-treatment baseline comparisons between the GGE and CTL groups. A summary table listing all of the trend effects of VPA administration is shown in Table 7.

4. Discussion

This is the first rs-fMRI study evaluating prospective network effects in FC of antiepileptic treatment in GGE. Epilepsy studies so far have evaluated either global connectivity differences when comparing antiepileptic medications (Hermans et al., 2015), or regional FC changes due to acute antiepileptic medication withdrawal in patients admitted to the epilepsy monitoring unit (Haneef et al., 2015). However, prospective scalp EEG connectivity studies have evaluated VPA treatment effects in GGE and of vagal nerve stimulation in people medically refractory epilepsies (Kay et al., 2013; Fraschini et al., 2014). This study utilizes a natural nonhuman primate model for GGE. Despite limitations related to the need for sedation for MRI, the lack of concurrent EEG recording, and the lack of correlation with seizure outcome, our resting-state fMRI platform not only confirmed baseline differences between epileptic and control baboons from a previous study (Salinas and Szabó, 2015), but also demonstrated significant changes occurring both acutely, after intravenous administration of valproic acid (20 mg/kg), as well as sub-acutely, following a seven day oral maintenance therapy (20–80 mg/kg). At baseline, cortico-cortical FC was overall increased, while thalamic FC was decreased in the GGE baboons. Acutely,

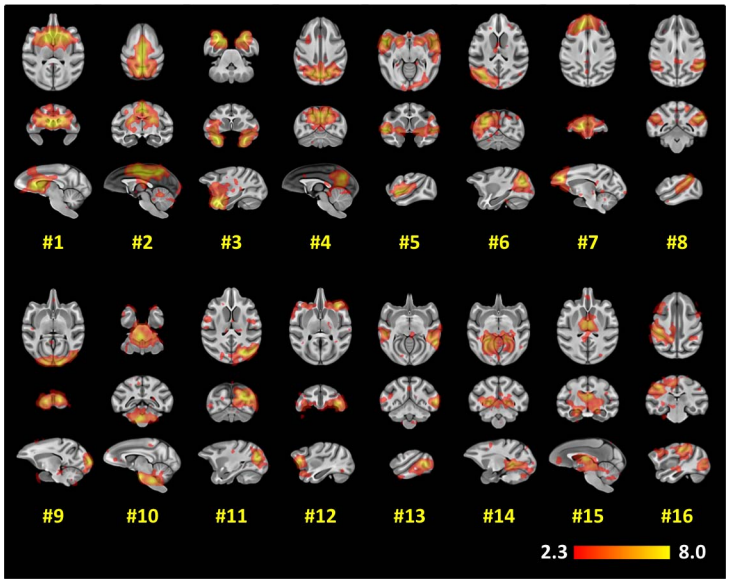

Fig. 2. Resting-state network maps determined by the spatial ICA of all subjects. Legend: Orthogonal slices of maximal response are shown. Each ICA map was thresholded at z > 4.00.

therapeutic VPA levels decreased cortico-cortical and increased sub-cortico-cortical connectivity. Most of these "acute" effects were not sustained after short-term oral VPA therapy resulting only in sub-therapeutic levels. Nonetheless, most of the baseline FC changes demonstrated by the GGE group had resolved after oral treatment when compared to the pre-treatment control group.

4.1. Baseline differences

The FC differences between GGE and CTL groups have been recently reported in a different cohort of baboons (Salinas and Szabó, 2015). The whole group ICA identified 16 networks compared to the 14 from the previous study, with eight networks overlapping and two additional networks demonstrating cortical maxima that were minimally displaced between the studies. Although our initial rs-fMRI study (Salinas and Szabó, 2015) had a larger sample size (N = 20; 10 GGE/10 CTL), in this rs-fMRI study, we excluded baboons with colpocephaly and/or occipital horn elongations, thereby increasing the structural homogeneity of our smaller sample size (N = 13; 7 GGE/6 CTL) and limiting any possibility of these scans skewing our FC results. Interestingly, the high coherence of ICA-derived brain networks between these two datasets suggests that the structural differences found in our first rs-fMRI study (Salinas and Szabó, 2015) had minimal impact on the functional brain networks obtained using ICA. Therefore, we are confident that the brain networks analyzed in both of our studies remain valid and integral to the assessment of FC in our baboon model of GGE. Changes in nomenclature were also due to the adaptation of a more formal and widely cited stereotactic atlas (Saleem and Logothetis, 2007). Nonetheless, similar to the previous study, FC was mostly increased in all of the altered networks, most cortico-cortical connections involving the parietal and visual cortices. The main difference between this rs-fMRI study and our previous study was decreased FC of the thalamus. This is consistent with a recent study showing decreased default mode network (DMN) connectivity to the thalamus in people with VPA-refractory GGE refractory (Kay et al., 2013), and microstructural changes in thalamo-cortical connections in diffusion tensor imaging (Vollmar et al., 2012).

4.2. Acute VPA effects

After the intravenous administration of a single loading dose of VPA, FC changes were noted in three networks with only one of those networks (i.e. the basal ganglia) demonstrating an increase in FC in the GGE group. Within one hour of intravenous administration of VPA, the levels reached mean concentrations of 82 mcg/ml (range: 51–99 mcg/

Table 2
ANOVA results of group, VPA dose, and their interactions for each of the ICA-derived intrinsic connectivity networks.

IC (#)	Intrinsic connectivity network	Baseline (GGE vs. CTL)		Acute VPA vs. baseline		Subacute VPA vs. baseline		GGE subacute VPA vs. CTL baseline	
		$F_{(1,29)}$	p-Value	$F_{(1,29)}$	p-Value	$F_{(1,29)}$	p-Value	$F_{(1,29)}$	p-Value
1	Basal ganglia	–	–	31.03	5.21×10^{-6}	–	–	–	–
2	Pericingulate	32.62	3.53×10^{-6}	–	–	–	–	–	–
3	Amygdala	–	–	–	–	–	–	–	–
4	Precuneus (i.e. DMN)	22.76	4.80×10^{-5}	–	–	–	–	–	–
5	Perisylvian operculum	–	–	–	–	–	–	38.82	8.48×10^{-7}
6	Left parieto-occipital	28.98	8.75×10^{-6}	–	–	–	–	–	–
7	Fronto-parietal	–	–	–	–	–	–	38.51	9.07×10^{-7}
8	Auditory	–	–	–	–	–	–	–	–
9	Primary visual	–	–	30.64	5.73×10^{-6}	–	–	–	–
10	Pons	–	–	–	–	–	–	–	–
11	Parietal	29.51	7.63×10^{-6}	21.47	7.01×10^{-5}	–	–	–	–
12	Orbitofrontal	30.44	6.03×10^{-6}	–	–	24.82	2.67×10^{-5}	–	–
13	Temporo-parietal	37.62	1.10×10^{-6}	–	–	–	–	–	–
14	Secondary (basal) visual area	29.93	6.86×10^{-6}	–	–	–	–	–	–
15	Thalamus	40.25	6.22×10^{-7}	–	–	–	–	–	–
16	Sensorimotor/visual	–	–	–	–	–	–	–	–

Table 3
Maximum cluster locations of functional connectivity differences between the GGE and CTL groups at baseline. †Labels correspond to the homologous areas in the rhesus (Saleem and Logothetis, 2007); DMN = default mode network; negative z-scores indicate cluster sizes being greater in the CTL than GGE group.

IC #	Seed region	Clusters		Local maxima					
		Voxels	p-Value	Region	Label†	Z-score	X (mm)	Y (mm)	Z (mm)
2	Pericingulate	2090	0.0253	Lateral orbital gyrus	Area 12o	4.22	21.6	11.4	− 2.4
		3079	0.0026	Thalamus	–	− 4.75	− 7.8	− 17.4	1.2
		2100	0.0247	Fundus of the superior temporal sulcus	Area FST	− 4.16	− 25.2	− 24.6	− 4.2
4	Precuneus (i.e. DMN)	6901	1.31×10^{-6}	Occipital gyrus	V2	4.97	− 6.0	− 39.0	4.8
		2355	0.0109	Ventral bank of the intraparietal sulcus	Lateral intraparietal area	− 4.16	19.2	− 24.6	13.8
6	Left parieto-occipital	7368	1.01×10^{-6}	Cerebellum	–	4.62	− 4.8	− 36.6	− 3.6
11	Parietal	3288	0.0013	Amygdala	Accessory basal nucleus	4.03	6.0	− 3.6	− 13.2
12	Orbitofrontal	3869	0.0006	Fundus of the intraparietal sulcus	Ventral intraparietal area	4.16	11.4	− 33.6	7.2
		2202	0.0204	Postcentral gyrus	Areas 3a/b	4.48	25.2	− 12.0	5.4
13	Temporo-parietal	2667	0.0051	Fundus of the superior temporal sulcus	Area FST	4.31	− 19.2	− 25.2	1.8
		1966	0.0283	Dorsal bank of the superior temporal sulcus	Area TPO	3.86	− 24.6	0.6	− 12.0
		15,231	5.62×10^{-12}	Posterior cingulate cortex	Area 23c	− 4.89	4.8	− 13.8	13.2
		1853	0.0379	Ventral bank of the intraparietal sulcus	Lateral intraparietal area	− 4.08	13.8	− 27.0	16.2
14	Secondary (basal) visual area	10,794	9.01×10^{-9}	Occipital gyrus	V2	4.44	− 6.0	− 41.4	0.6
		1913	0.0448	Dorsal bank of the superior temporal sulcus	Area TPO	4.37	− 29.4	− 15.0	− 5.4
15	Thalamus	16,264	3.78×10^{-12}	Thalamus	–	− 4.70	− 9.6	− 18.6	1.8

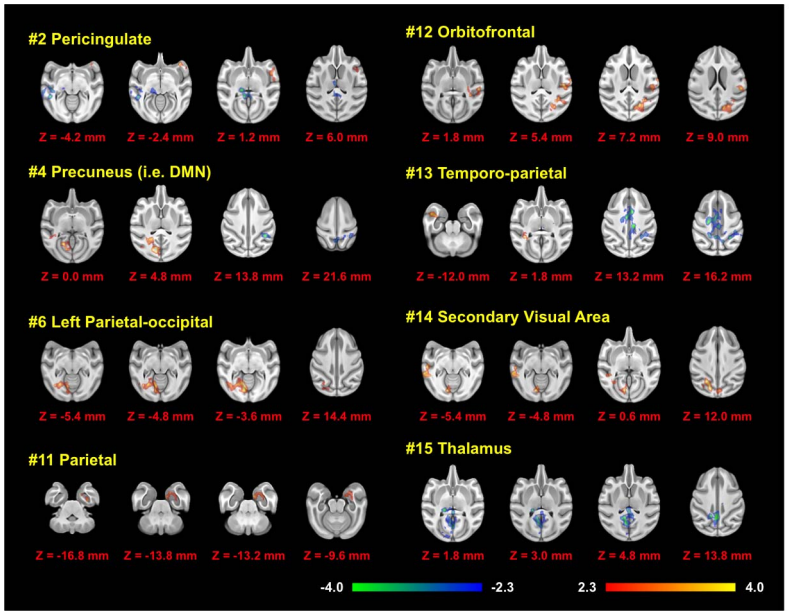

Fig. 3. Functional connectivity differences between the GGE and CTL group's baseline scans.

ml), reflecting therapeutic levels in humans. Presumably, networks with increased, or even altered, FC at baseline should subserve the epileptic network. However, it is likely that the effects of acute VPA therapy, which reduces cortical excitability via interactions with ion channels and increasing GABA, is more likely to demarcate the epileptic network. This is particularly clear with respect to the increased connectivity of the basal ganglia network, targeting the medial frontal lobe, cingulate cortex, postcentral central gyrus, occipital lobe and cerebellum, including brain regions associated with the epileptic network underlying juvenile myoclonic epilepsy (JME; Vollmar et al., 2012; Kay et al., 2013). Increased basal ganglia connectivity (due to acute VPA administration) is in line with the facilitation of a subcortical inhibitory effect via the striatum—in particular, the substantia nigra pars reticulata—over parts of the epileptic network (Gale, 1992; Paz et al., 2007). On the other hand, the FC of the parietal network is decreased in the GGE group (compared to the CTL group) in this network's

Table 4
Maximum cluster locations of functional connectivity differences between the GGE and CTL groups after acute VPA administration. †Labels correspond to the homologous areas in the rhesus (Saleem and Logothetis, 2007); negative z-scores indicate cluster sizes being greater in the CTL than GGE group.

IC #	Seed region	Clusters		Local maxima					
		Voxels	p-Value	Region	Label	Z-score	X (mm)	Y (mm)	Z (mm)
1	Basal ganglia	6286	3.34×10^{-6}	Midcingulate cortex	Area 24c′	4.42	5.4	− 6.0	15.0
		3839	0.0004	Occipital gyrus	V2	4.13	− 0.6	− 46.8	0.6
9	Primary visual	2538	0.0179	Occipital gyrus	V1	− 4.52	− 12.0	− 36.6	1.2
11	Parietal	2871	0.0020	Posterior orbital gyrus	Area 13m	− 3.75	8.4	11.4	4.2
		2095	0.0145	Middle temporal gyrus	Area TEO	− 3.89	27.6	− 28.8	− 1.2

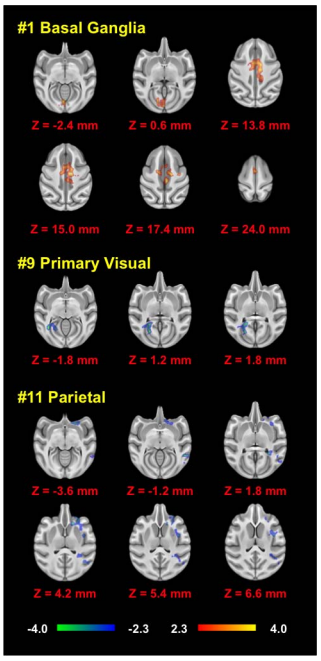

Fig. 4. Functional connectivity differences between the GGE and CTL group's after acute administration of VPA.

connections to the orbital cortex, insula and claustrum, occipital lobes, lateral temporal lobes, and the thalamus—all of which are identified as nodes of the epileptic network using functional neuroimaging and intracranial EEG in the baboons (Szabó et al., 2008; Szabó et al., 2012b). The presumed therapeutic benefit of increasing FC of the basal ganglia network is likely to reduce seizure expression, while the reduction of FC in the parietal and primary visual cortices may inhibit seizure generation. EEG-fMRI can temporally elucidate these processes, and blood flow changes predominating in the posterior head regions have been shown to precede spike-and-wave discharges in human absence epilepsy (Benuzzi et al., 2012).

4.3. Subacute VPA effects

After one week of oral VPA treatment, few changes were noted in the GGE group relative to the control baboons compared to baseline, which may not be surprising since the total VPA levels ended up in the subtherapeutic range (mean = 12 mcg/ml, range: 5–21 mcg/ml). The network FC changes with acute VPA therapy were no longer apparent, and overall there was no difference with respect to baseline. The only FC change involved the orbitofrontal network showing increased connectivity with respect to the primary sensory cortices. While the orbitofrontal cortices and primary sensory cortices have been implicated in the epileptic network in animal models and human GGE, the therapeutic effect in modulation of this pathway is unclear, and should be evaluated using cortico-cortical evoked potentials (Szabó et al., 2012b). Comparison of the FC after subacute therapy in the GGE group with the pre-treatment controls, however, reflected some degree of

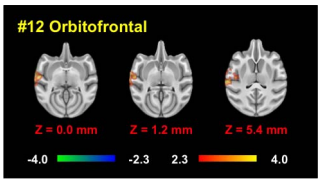

Fig. 5. Functional connectivity differences between the GGE and CTL group's after subacute administration of VPA.

normalization of the altered baseline FC associated with epilepsy and restoration of physiological connectivity in the GGE group. Increased FC in the perisylvian network with parietal lobe targets may represent parts of the epileptic network not effectively suppressed by subtherapeutic doses of VPA or a functional benefit of treatment. The overall decreased difference between these groups may be related to global VPA effects on cerebral blood flow(Gaillard et al., 1996), but the regional decrease of FC of the frontoparietal network, on the other hand, may reflect previously reported seizure-induced injury in the sensorimotor cortices (Young et al., 2013).

4.4. Shortfalls and advantages

There are several potential shortfalls of this study. The first shortfall is the lack of correlation of our fMRI signals with simultaneously recorded scalp EEG. EEG-fMRI studies in focal epilepsies have been utilized to evaluate resting-state FC within the epileptic network (van Houdt et al., 2015; Iannotti et al., 2016) and in intrinsic connectivity (IC) networks (Shamshiri et al., 2017). While the first two studies showed transient increases in the BOLD signal during IEDs, overall, the resting-state connectivity within the epileptic network was maintained even in the absence of IEDs (van Houdt et al., 2015; Iannotti et al., 2016). On the other hand, the attentional and visual IC networks were similar to controls in focal epilepsy patients in IED-free periods (Shamshiri et al., 2017). Based upon these observations, FC changes within the epileptic network in patients with medically refractory focal epilepsy are due to underlying developmental or seizure-related plasticity, whereas the epileptic network appears to disrupt other physiological networks. In people with GGE, on the other hand, the underlying etiology or mechanism is unknown. One EEG-fMRI study in people with GGE, however, showed that FC was not altered in IED-free periods in selected brain regions associated with cortical regions activated during generalized spike-and-wave discharges (Moeller et al., 2011). Based upon these findings, the authors suggested that the epileptic network and its connections to other networks were not altered. However, evidence of multiregional interictal epileptic discharges on intracranial EEG in the epileptic baboon suggest more widespread cortical abnormalities which, in addition to generalized spike-and-wave complexes, can contribute to FC changes that cannot be correlated with scalp EEG (Szabó et al., 2012b). Furthermore, it is not clear whether brain regions expressing generalized spike-and-wave complexes are the same as those underlying their generation, as FC is more likely to be altered in the latter. Nonetheless, correlation of a treatment-related FC response to generalized IED rate with EEG-fMRI would add to our understanding of the connections underlying the generation and

Table 5
Maximum cluster locations of functional connectivity differences between the GGE and CTL groups after subacute VPA administration. †Labels correspond to the homologous areas in the rhesus (Saleem and Logothetis, 2007); negative z-scores indicate cluster sizes being greater in the CTL than GGE group.

IC #	Seed region	Clusters		Local maxima					
		Voxels	p-Value	Region	Label	Z-score	X (mm)	Y (mm)	Z (mm)
12	Orbitofrontal	6331	1.37×10^{-6}	Postcentral gyrus	Areas 1–2	4.67	− 34.8	− 14.4	5.4
				Postcentral gyrus	Areas 1–2	4.44	− 35.4	− 6.6	0.0
				Postcentral gyrus	Areas 3a/b	4.35	− 29.4	− 9.0	1.2

Table 6
Cluster locations of functional connectivity differences between the GGE subacute VPA and CTL baseline scan. †Labels correspond to the homologous areas in the rhesus (Saleem and Logothetis, 2007); negative z-scores indicate cluster sizes being greater in the CTL than GGE group.

IC #	Seed region	Clusters		Local maxima					
		Voxels	p-Value	Region	Label	Z-score	X (mm)	Y (mm)	Z (mm)
5	Perisylvian Operculum	3520	0.0013	Postcentral gyrus	Areas 1–2	4.46	− 31.2	− 7.2	10.8
				Inferior parietal lobule	Area 7b	4.06	− 30.6	− 16.8	9.0
				Postcentral gyrus	Areas 3a/b	3.41	− 34.2	− 4.8	2.4
7	Fronto-parietal	7477	7.75×10^{-7}	Postcentral gyrus	Areas 1–2	− 4.53	− 30.0	1.2	− 3.0
				Postcentral gyrus	Areas 1–2	− 4.26	− 24.6	1.2	− 3.0
				Frontal operculum	Frontal area F5	− 3.95	− 27.6	4.8	5.4
				Agranular insular cortex	Lateral agranular insula area	− 3.90	− 19.2	5.4	− 3.0
				Superior temporal gyrus/auditory cortex	Medial rostrotemporal, belt region of the auditory cortex	− 3.77	− 24.0	− 1.8	− 8.4
				Frontal operculum	Precentral opercular area	− 3.72	− 28.8	8.4	− 4.2

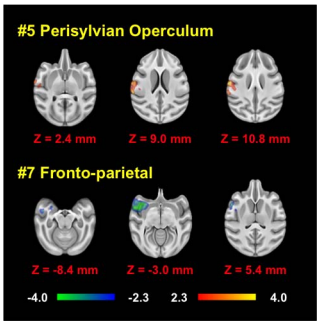

Fig. 6. Functional connectivity differences between the GGE group's subacute VPA and the CTL group's baseline scans.

secondary effects of generalized spike-and-wave complexes (Centeno and Carmichael, 2014).

The second issue includes medication effects on global or network FC. In the same fashion, VPA has been shown to decrease cerebral blood flow in humans both globally and regionally, FC may also be altered in baboons (Gaillard et al., 1996). In terms of group comparisons, the same dose of ketamine was maintained for both groups using continuous intravenous infusions, and for VPA therapy. At each time-point (acute and subacute), FC changes in epileptic baboons were compared not only to the baseline values, but also relative to the FC changes for the same time-points in the control animals. Hence, we expect to have minimized the variable effects of these drugs on global and network connectivity. While some of the FC changes may be affected by the CTL group, the main affects on FC were presumed to be driven by the epileptic networks (activated by ketamine) and their response to VPA. Again, scalp EEG recordings, particularly EEG-fMRI would help elucidate to what extent ictal on interictal discharges may be affecting FC in the GGE group.

The third shortcoming of this study was that the VPA doses were subtherapeutic after a week of oral therapy and that in such a short period the clinical response to VPA cannot be measured in order to determine whether the doses were actually therapeutic. Based upon the data obtained during this study, we realize that much higher maintenance doses of VPA will be required to achieve optimal clinical effects in future studies.

On the other hand, the assessment of intra-network FC changes with treatment demonstrated significant findings (even in a study with such a small sample size), with many of these FC changes occurring in brain regions, which are linked to the underlying pathophysiology of GGE. We acknowledge that in this study we are only assessing the intra-network FC changes, we do plan to report on the between-network FC changes (using graph theoretical analysis) in an upcoming research manuscript.

Table 7
Summary table of the effects of VPA dose for each of the ICA-derived intrinsic connectivity networks.

IC (#)	Intrinsic connectivity network	Acute VPA vs. baseline	Subacute VPA vs. baseline	EPI subacute VPA vs. CTL baseline
1	Basal ganglia	↑ Midcingulate cortex ↑ Postcentral gyrus ↑ Dorsal basal nuclei ↑ Medial superior frontal gyrus ↑ Occipital gyrus ↑ Cerebellum	–	–
5	Perisylvian operculum	–	–	↑ Postcentral gyrus ↑ Inferior parietal lobule
7	Fronto-parietal	–	–	↓ Postcentral gyrus ↓ Frontal operculum ↓ Agranular insular cortex ↓ Superior temporal gyrus/auditory cortex ↓ Frontal operculum
9	Primary visual	↓ Occipital gyrus ↓ Retrosplenial cortex	–	–
11	Parietal	↓ Posterior orbital gyrus ↓ Granular insular cortex ↓ Agranular insular cortex ↓ Middle temporal gyrus ↓ Thalamus ↓ Dorsal bank of the superior temporal sulcus ↓ Occipital gyrus	–	–
12	Orbitofrontal	–	↑ Postcentral gyrus	–

The advantage of the baboon model is its similarity to human GGE (particularly JME) even in its response to antiepileptic medications (Szabó et al., 2009; Szabó et al., 2013). Even though we utilized ketamine for sedation, this imaging platform in the epileptic baboon is not affected by interactions with other antiepileptic medications, concerns over the subject's attentiveness while in the scanner, time restrictions which limit rs-fMRI scan length, and the reproducibility of the rs-fMRI data. While baboons have similar brain structure and function to humans, their simpler cortical anatomy may underlie more robust intergroup comparisons. These factors may explain our ability to rely solely on a data-driven approach, avoiding any potential bias in seed selection.

5. Conclusions

While most authors define the epileptic network underlying GGE in humans as the thalamocortical pathways connecting the medial thalamus with the frontal cortices (Moeller et al., 2008; Vollmar et al., 2012), it is evident from this baboon model of GGE (Szabó et al., 2008; Salinas and Szabó, 2015) and human fMRI studies (Benuzzi et al., 2012; Kay et al., 2013) that the epileptic network depends on more extensive cortico-cortical and cortico-subcortical interactions. To what extent and how the epileptic network “hijacks” these physiological networks needs more investigation, including EEG-fMRI analysis. It is also possible that the generalized ictal discharges generated within the epileptic network are in response to the altered FC of these physiological networks. While this study does not conclusively demonstrate which pathways need to be effectively modulated by antiepileptic treatment to render a patient seizure free and restore optimal physiological interactions, it does demonstrate the feasibility of utilizing rs-fMRI to potentially measure a therapeutic response of novel antiepileptic treatments.

Supplementary data to this article can be found online at http://dx.doi.org/10.1016/j.nicl.2017.07.013.

Conflict of interest statement

There was no conflict of interest to report by either author.

Acknowledgements

This study was supported by National Institutes of Health (R21-NS084198) and utilized the primate resources of the Texas Biomedical Research Institute in San Antonio, Texas, which is supported by the Research Facilities Improvement Grants (C06-RR013556; C06-RR014578; C06-RR015456). We would like to thank 1) Dr. Jinqi Li from UTHSCSA's Research Imaging Institute for MRI acquisition and 2) Katie Strychalski and Devon Klipsic, D.V.M. from UTHSCSA's Laboratory Animal Resources for animal support throughout the study.

References

Beckmann, C.F., DeLuca, M., Devlin, J.T., Smith, S.M., 2005. Investigations into resting-state connectivity using independent component analysis. Philos. Trans. Biol. Sci. 360, 1001–1013.

Benuzzi, F., Mirandola, L., Pugnaghi, M., Farinelli, V., Tassinari, C.A., Capovilla, G., Cantalupo, G., Beccaria, F., Nichelli, P., Meletti, S., 2012. Increased cortical bold signal anticipates generalized spike and wave discharges in adolescents and adults with idiopathic generalized epilepsies. Epilepsia 53, 622–630.

Centeno, M., Carmichael, D.W., 2014. Network connectivity in epilepsy: resting state fMRI and EEG-fMRI contributions. Front. Neurol. 5, 93.

Chai, X.J., Castanon, A.N., Ongur, D., Whitfield-Gabrieli, S., 2012. Anticorrelations in resting state networks without global signal regression. NeuroImage 59, 1420–1428.

Chen, G., Xie, C., Ward, B.D., Li, W., Antuono, P., Li, S.J., 2012. A method to determine the necessity for global signal regression in resting-state fMRI studies. Magn. Reson. Med. Off. J. Soc. Magn. Reson. Med./Soc. Magn. Reson. Med. 68, 1828–1835.

Clemens, B., Puskas, S., Besenyei, M., Kovacs, N.Z., Spisak, T., Kis, S.A., Emri, M., Hollody, K., Fogarasi, A., Kondakor, I., Fekete, I., 2014. Valproate treatment normalizes eeg functional connectivity in successfully treated idiopathic generalized epilepsy patients. Epilepsy Res. 108, 1896–1903.

Fraschini, M., Demuru, M., Puligheddu, M., Floridia, S., Polizzi, L., Maleci, A., Bortolato, M., Hillebrand, A., Marrosu, F., 2014. The re-organization of functional brain networks in pharmaco-resistant epileptic patients who respond to vns. Neurosci. Lett. 580, 153–157.

Gaillard, W.D., Zeffiro, T., Fazilat, S., DeCarli, C., Theodore, W.H., 1996. Effect of valproate on cerebral metabolism and blood flow: an 18f-2-deoxyglucose and 15o water positron emission tomography study. Epilepsia 37, 515–521.

Gale, K., 1992. Subcortical structures and pathways involved in convulsive seizure generation. J. Clin. Neurophysiol. Off. Publ. Am Electroencephalographic Soc. 9, 264–277.

Haneef, Z., Levin, H.S., Chiang, S., 2015. Brain graph topology changes associated with anti-epileptic drug use. Brain Connectivity 5, 284–291.

Harding, G.F., Edson, A., Jeavons, P.M., 1997. Persistence of photosensitivity. Epilepsia 38, 663–669.

Hermans, K., Ossenblok, P., van Houdt, P., Geerts, L., Verdaasdonk, R., Boon, P., Colon, A., de Munck, J.C., 2015. Network analysis of eeg related functional MRI changes due to medication withdrawal in focal epilepsy. NeuroImage. Clin. 8, 560–571.

van Houdt, P.J., Ossenblok, P.P., Colon, A.J., Hermans, K.H., Verdaasdonk, R.M., Boon, P.A., de Munck, J.C., 2015. Are epilepsy-related fMRI components dependent on the presence of interictal epileptic discharges in scalp eeg? Brain Topogr. 28, 606–618.

Iannotti, G.R., Grouiller, F., Centeno, M., Carmichael, D.W., Abela, E., Wiest, R., Korff, C., Seeck, M., Michel, C., Pittau, F., Vulliemoz, S., 2016. Epileptic networks are strongly connected with and without the effects of interictal discharges. Epilepsia 57, 1086–1096.

Kay, B.P., DiFrancesco, M.W., Privitera, M.D., Gotman, J., Holland, S.K., Szaflarski, J.P., 2013. Reduced default mode network connectivity in treatment-resistant idiopathic generalized epilepsy. Epilepsia 54, 461–470.

Löscher, W., 2002. Basic pharmacology of valproate: a review after 35 years of clinical use for the treatment of epilepsy. CNS Drugs 16, 669–694.

Love, S.A., Marie, D., Roth, M., Lacoste, R., Nazarian, B., Bertello, A., Coulon, O., Anton, J.L., Meguerditchian, A., 2016. The average baboon brain: MRI templates and tissue probability maps from 89 individuals. NeuroImage 132, 526–533.

Moeller, F., Siebner, H.R., Wolff, S., Muhle, H., Boor, R., Granert, O., Jansen, O., Stephani, U., Siniatchkin, M., 2008. Changes in activity of striato-thalamo-cortical network precede generalized spike wave discharges. NeuroImage 39, 1839–1849.

Moeller, F., Maneshi, M., Pittau, F., Gholipour, T., Bellec, P., Dubeau, F., Grova, C., Gotman, J., 2011. Functional connectivity in patients with idiopathic generalized epilepsy. Epilepsia 52, 515–522.

National Research Council, 2011. Guide for the care and use of laboratory animals. In: Animals. The National Academies Press, Washington, D.C C.f.t.U.o.t.G.f.t.C.U.o.L.

Paz, J.T., Chavez, M., Saillet, S., Deniau, J.M., Charpier, S., 2007. Activity of ventral medial thalamic neurons during absence seizures and modulation of cortical paroxysms by the nigrothalamic pathway. J. Neurosci. Off. J. Soc. Neurosci. 27, 929–941.

Perucca, E., 2002. Pharmacological and therapeutic properties of valproate: a summary after 35 years of clinical experience. CNS Drugs 16, 695–714.

Pflanz, C.P., Pringle, A., Filippini, N., Warren, M., Gottwald, J., Cowen, P.J., Harmer, C.J., 2015. Effects of seven-day diazepam administration on resting-state functional connectivity in healthy volunteers: a randomized, double-blind study. Psychopharmacology 232, 2139–2147.

Saleem, K.S., Logothetis, N.K., 2007. A Combined MRI and Histology Atlas of the Rhesus Monkey Brain in Stereotaxic Coordinates. Academic Press, London.

Salinas, F.S., Szabó, C.Á., 2015. Resting-state functional connectivity in the baboon model of genetic generalized epilepsy. Epilepsia.

Shamshiri, E.A., Tierney, T.M., Centeno, M., St Pier, K., Pressler, R.M., Sharp, D.J., Perani, S., Cross, J.H., Carmichael, D.W., 2017. Interictal activity is an important contributor to abnormal intrinsic network connectivity in paediatric focal epilepsy. Hum. Brain Mapp. 38, 221–236.

Smith, S.M., 2002. Fast robust automated brain extraction. Hum. Brain Mapp. 17, 143–155.

Smith, S.M., Jenkinson, M., Woolrich, M.W., Beckmann, C.F., Behrens, T.E.J., Johansen-Berg, H., Bannister, P.R., Luca, M.D., Drobnjak, I., Flitney, D.E., Niazy, R.K., Saunders, J., Vickers, J., Zhang, Y., Stefano, N.D., Brady, J.M., Matthews, P.M., 2004. Advances in functional and structural MR image analysis and implementation as FSL. NeuroImage 23 (Suppl. 1), S208–219.

Sundqvist, A., Nilsson, B.Y., Tomson, T., 1999. Valproate monotherapy in juvenile myoclonic epilepsy: dose-related effects on electroencephalographic and other neurophysiologic tests. Ther. Drug Monit. 21, 91–96.

Szabó, C.Á., Narayana, S., Franklin, C., Knape, K.D., Davis, M.D., Fox, P.T., 2008. “Resting” CBF in the epileptic baboon: correlation with ketamine dose and interictal epileptic discharges. Epilepsy Res. 82, 57–63.

Szabó, C.Á., Leland, M.M., Knape, K.D., Williams, J.T., 2009. The baboon model of epilepsy: current applications in biomedical research. In: Van de Berg, J.L., Williams-Blangero, S., Tardif, S.D. (Eds.), The Baboon in Biomedical Research. Springer-Verlag, New York, pp. 351–370.

Szabó, C.Á., Salinas, F.S., Narayana, S., 2011. Functional pet evaluation of the photosensitive baboon. Open Neuroimaging J. 5, 206–215.

Szabó, C.Á., Knape, K.D., Leland, M.M., Cwikla, D.J., Williams-Blangero, S., Williams, J.T., 2012a. Epidemiology and characterization of seizures in a pedigreed baboon colony. Comp. Med. 62, 535–538.

Szabó, C.Á., Salinas, F.S., Leland, M.M., Caron, J.-L., Hanes, M.A., Knape, K.D., Xie, D., Williams, J.T., 2012b. Baboon model of generalized epilepsy: continuous intracranial video-EEG monitoring with subdural electrodes. Epilepsy Res.

Szabó, C.Á., Knape, K.D., Leland, M.M., Williams, J.T., 2013. Electroclinical phenotypes in a pedigreed baboon colony. Epilepsy Res. 105, 77–85.

Szabó, C.Á., De La Garza, M., Rice, K., Bazan Iii, C., Salinas, F.S., 2016. Relationship between epilepsy and colpocephaly in baboons (*Papio hamadryas*). Comp. Med. 66, 241–245.

U.S. Public Health Service, 2009. Animal Welfare Act and Animal Welfare Regulations. U.S. Dept. of Agriculture, Animal and Plant Health Inspection Service, Washington, D.C.

Vollmar, C., O'Muircheartaigh, J., Symms, M.R., Barker, G.J., Thompson, P., Kumari, V., Stretton, J., Duncan, J.S., Richardson, M.P., Koepp, M.J., 2012. Altered microstructural connectivity in juvenile myoclonic epilepsy: the missing link. Neurology 78, 1555–1559.

Wang, L., Xia, M., Li, K., Zeng, Y., Su, Y., Dai, W., Zhang, Q., Jin, Z., Mitchell, P.B., Yu, X., He, Y., Si, T., 2015. The effects of antidepressant treatment on resting-state functional brain networks in patients with major depressive disorder. Hum. Brain Mapp. 36, 768–778.

Weissenbacher, A., Kasess, C., Gerstl, F., Lanzenberger, R., Moser, E., Windischberger, C., 2009. Correlations and anticorrelations in resting-state functional connectivity MRI: a quantitative comparison of preprocessing strategies. NeuroImage 47, 1408–1416.

Woolrich, M.W., Jbabdi, S., Patenaude, B., Chappell, M., Makni, S., Behrens, T., Beckmann, C., Jenkinson, M., Smith, S.M., 2009. Bayesian analysis of neuroimaging data in FSL. NeuroImage 45, S173–186.

Young, N.A., Szabó, C.Á., Phelix, C.F., Flaherty, D.K., Balaram, P., Foust-Yeoman, K.B., Collins, C.E., Kaas, J.H., 2013. Epileptic baboons have lower numbers of neurons in specific areas of cortex. Proc. Natl. Acad. Sci. U.S.A. 110 (47), 19107–19112. http://dx.doi.org/10.1073/pnas.1318894110.

Yang, R., Zhang, H., Wu, X., Yang, J., Ma, M., Gao, Y., Liu, H., Li, S., 2014. Hypothalamus-anchored resting brain network changes before and after sertraline treatment in major depression. Biomed. Res. Int. 2014, 915026.

Youngblood, M.W., Chen, W.C., Mishra, A.M., Enamandram, S., Sanganahalli, B.G., Motelow, J.E., Bai, H.X., Frohlich, F., Gribizis, A., Lighten, A., Hyder, F., Blumenfeld, H., 2015. Rhythmic 3-hz discharge is insufficient to produce cortical bold fMRI decreases in generalized seizures. NeuroImage 109, 368–377.

Zhang, Y., Brady, M., Smith, S., 2001. Segmentation of brain MR images through a hidden Markov random field model and the expectation-maximization algorithm. IEEE Trans. Med. Imaging 20, 45–57.